Investigation of Rotational Relaxation by Double Resonance and Stark Switch Techniques

W. Schrepp, H. Dreizler, and A. Guarnieri
Abteilung Chemische Physik im Institut für Physikalische Chemie der Universität Kiel

Z. Naturforsch. **35a**, 832–840 (1980); received May 22, 1980

For the four rotational levels $J_{K_-K_+} = 1_{01}, 1_{10}, 2_{12}$ and 2_{21} of ethylene oxide all possible four level double resonance experiments for dipole allowed transitions have been performed to investigate collisional effects and to determine the relative change of signal intensity, $\eta = \Delta I/I$, due to high power pump radiation. The T_1- and T_2-relaxation times have been measured for all dipole allowed transitions within these four levels.

A combination of the data obtained from both experimental methods allows the determination of rate and bath constants taking into account only first order dipolar transitions. No further restrictions have been used. This approximation is supported by a triple resonance experiment.

In addition to the pure gas investigation in the absence of external fields, rotational relaxation has been studied in the presence of a static electric field and in a mixture with hydrogen.

Introduction

We report an investigation of the rotational relaxation of ethylene oxide, C_2H_4O. Two experimental methods were used: I) four level double resonance [1, 2, 3] in the frequency domain and II) two level transient Stark-switch technique in the time domain [4, 5, 6]. Our aim is the determination of the rate constants.

The principles of the two methods are illustrated by Figs. 1 and 2. The four level double resonance gives the relative change of a signal absorption, $\eta = \Delta I/I$, by collision induced transitions. η measures the strength of these transitions. By Stark-switch experiments we determine the relaxation times T_1 and T_2, which phenomenologically describe the decay of the disturbed population difference ΔN in an ensemble of two level systems to its Boltzmann equilibrium value and the decay of the induced macroscopic polarisation to a negligible value* zero, respectively.

η, T_1 and T_2 can be related under suitable assumptions to combinations of rate constants [1, 7, 8, 9]. Details for the relations to η are given in references [1, 9]. For linear molecules Liu et al. [7] derived the relations to T_1 and T_2. As has been shown, these relations can be extended to asymmetric top molecules [10].

The T_2-values reported in this work have not been used for the determination of the inelastic rate constants. They were measured because T_2 can be related to linewidth measurements [4]. Further the theoretical prediction [7] of $T_1 \simeq T_2$ should be confirmed.

As a rotational spectrum arises from a large number of populated levels, rotational relaxation is determined by even more rate constants. A considerable simplification can be obtained [1] by considering only effects in a selected four level scheme and treating the other populated levels as a thermal bath. For further simplification we analysed the measurements only in terms of the four first order

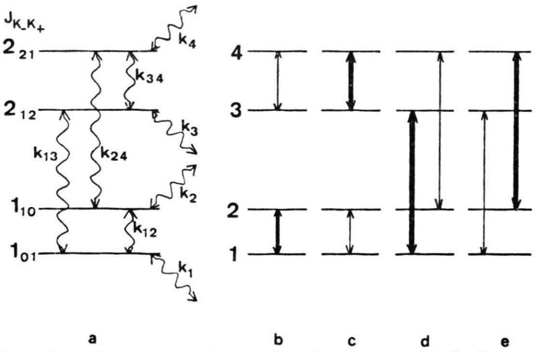

Fig. 1a. Investigated four level system of ethylene oxide ⇝ collisional transitions, characterized by rate constants k_{ij} connected to dipolar type transitions and bath constants k_i.

Fig. 1b–d. Possible four level double resonances ⟷ pump transitions with MW-power in the order of Watts, ↔ signal transitions with MW-power in the order of Microwatts. For each signal transition T_1 and T_2 may be determined.

Reprint request to Prof. Dr. H. Dreizler, Institut für Physikalische Chemie der Universität Kiel, Olshausenstr. 40–60 D-2300 Kiel.

* see Ref. [34].

0340-4811 / 80 / 0800-0832 $ 01.00/0. — Please order a reprint rather than making your own copy.

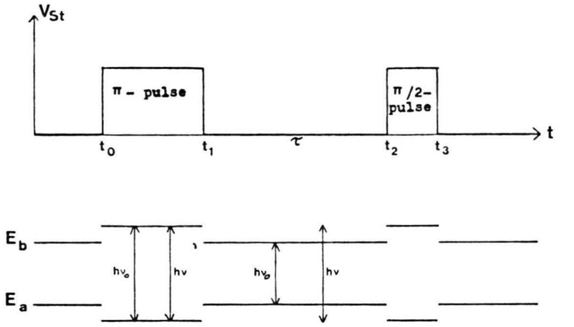

Fig. 2. Scheme for T_1-measurement. At t_0 the ensemble of two-level systems a, b is brought into resonance with the continously applied MW-field (h ν) by applying a Stark π-pulse. At t_1 the Stark voltage is switched off. In the following non-resonant period τ ΔN relaxes. At t_2 the system is brought into resonance again by a second Stark $\pi/2$-pulse [5, 6].

b-type dipolar collisional transitions or of the corresponding rate constants k_{ij} as indicated in Figure 1. Four "bath" constants k_i, sums of rate constants, describe the coupling of population variations to the bath. These were not assumed to be necessarily of dipolar type.

Figures 1 b—e give the four possible choices for the MW-pump and signal*. So it was possible to measure four η-values and four T_1- (and T_2-)values, which were sufficient to determine the eight inelastic rate and bath constants. Up to now the two types of measurements have been analysed separately for some molecules under more stringent assumptions because of the lack of experimental information. So the bath constants have been assumed to be equal, which may be an insufficient approximation as resulted from our analysis. The rate constants k_{ij} depend on these assumptions.

As there is still a discussion [1, 7, 11] of the $|m|$-dependence** of relaxation effects, most of the measurements were made without and with an external electric DC-field to lift the $|m|$-degeneracy of the rotational levels.

The four level double resonances showed a change of the magnitude but not of the sign of η. This is in contrast to the sign change observed in OCS [12, 13]. Within experimental accuracy no $|m|$-dependence of T_1 and T_2 has been found. Different results for NH_3 were reported by Hoke et al [14].

Experimental and Apparatus for Four Level Double Resonances

Ethylene oxide was supplied by J. T. Baker Chemical Co. with a purity of 99.7% and used after vacuum distillation.

The pressure was measured with a MKS Baratron 310 capacitance manometer. The influence of selective adsorption was reduced by a vacuum tank of 20 l which also increased the pressure stability.

For the double resonance experiment a resonant high power microwave radiation of frequency ν_p has to be applied. Due to this pump radiation the population difference of the pump transition levels is changed with respect to the thermal equilibrium. This change is transferred to other levels by molecular and wall collisions. The collisional transfer to two selected levels is monitored by a microwave of weak power and frequency ν_s. I is the peak intensity of the monitored signal transition, ΔI its pump and collisional induced change in intensity giving the $\eta = \Delta I / I$ value.

The frequencies of the investigated transitions are given in Table 1.

For the experiment with the selection of pump and signal frequency of Fig. 1 b we used the sensitive method of *m*icrowave *m*odulated *d*ouble *r*esonance (MMDR) [2, 9, 15, 16] with double modulation and demodulation. The general set up is given in Figure 3 a. A PIN-diode switches at 7 Hz the pump microwave on and off. In addition 33 kHz Stark modulation is applied*. With the first PSD I, with the second ΔI are measured. The pump was set off resonant when measuring I. The measurement of ΔI has to be carried out with a sufficient bandwidth of the detection system. For scaling of ΔI and I the gain of the second PSD has to be calibrated.

The phase stabilised pump source was a microwave sweeper (Hewlett-Packard 8690 B + 8694 A) in X-Band followed by a TWT-amplifier (Hughes

Tab. 1. Transitions and frequencies of ethylene oxide investigated in this work.

$J_{K_-K_+}$	$-J'_{K'_-K'_+}$	ν [MHZ]
1_{10}	-1_{01}	11385.71
2_{21}	-2_{12}	34157.13
2_{21}	-1_{10}	90548.93
2_{12}	-1_{01}	67777.51
3_{30}	-3_{21}	23134.32

---

* This procedure is in general not possible for symmetric top or linear molecules, as the selection rules are different.

** We use m for the magnetic quantum number.

* Attempts to measure I by means of three level double resonance [17] failed.

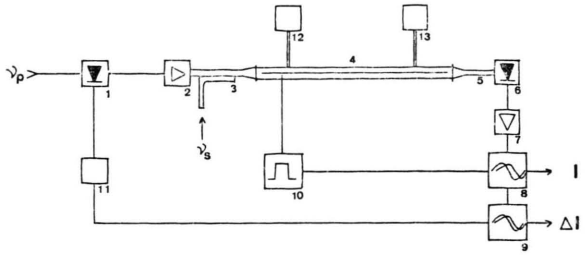

Fig. 3a. Scheme of the double modulation spectrometer for the measurement of $\eta = \Delta I/I$. The intensity I of the signal line is measured by 33 kHz Stark modulation, the change ΔI of intensity by 7 Hz on-off modulation of the pump radiation. ν_p and ν_s phase stabilized pump and signal radiation, 1 PIN-modulator 7 Hz, 2 TWT amplifier, 3 directional coupler, 4 Stark absorption cell, 5 m X-band, 5 cut off filter, 6 MW detector, 7 preamplifier, 8 phase sensitive detector for 33 kHz, 9 phase sensitive detector for 7 Hz. 10 Stark-Generator 33 kHz, 11 PIN-driver, 12 Capacitance manometer, 13 Vacuum tank, 20 *l*.

Fig. 3b. Scheme for the measurement of η with a cw pump source either resonant ($I + \Delta I$) or off resonant (I). Part 1,9 and 11 is omitted.

177H/771-HD). For the phase stabilised signa source a V-Band microwave sweeper (Hewlett-Packard 8690B + 8697A) was used. A special directional coupler [18] combined the radiations.

For the $|m|$-resolved measurements DC-voltages up to 2000 V/cm were applied to the Stark septum to lift the degeneracy. For the experiments according to Figs. 1c—e we used the procedure described by Oka [1]. The peak intensity I of the signal transition is determined by Stark spectroscopy with the pump microwave off resonant. We found that an off-set of 30 to 50 MHz is enough to avoid an observable collisional effect for pump powers in the order of Watt and pressures near 20 mT. When the pump frequency is tuned to resonance, the intensity is changed to $I + \Delta I$, if collisional effects are present. The apparatus is shown in Figure 3b. As pump sources OKI klystrons 35 V 12 (33 to 37 GHz, 700 mW), KA 701 A (68—72 GHz, 400 mW) and 90 V 11 (85—95 GHz, 120 mW) were used with phase stabilisation referenced to frequency standards Rhode and Schwarz XUC (470—1000 MHz) or Schomandl ND 800M (600—800 MHz). For the high frequency klystrons a two step stabilisation was necessary. The same klystrons or microwave sweepers were also used as signal sources.

Pump and signal radiations were combined by a commercial 10 dB directional coupler (Fig. 1c) or by a magic T with one adjustable short (Figure 1d, 1e).

The absorption cell was an usual 5 m X-band stark cell (Fig. 1c) or a 1.5 m stripline cell (Fig. 1d, 1e) [16, 19]. To prevent the pump radiation from reaching the signal source and the detector low pass filters, waveguide cut off filters and isolators were inserted. For the case of Fig. 1c with $\nu_p > \nu_s$ a coaxial cable attenuated the pump power sufficiently. The adjustment of the detector, for the corresponding wavelength separated for the case of Fig. 1e pump from signal radiation. For detection at 34 and 11 GHz commercial detector mountings with diodes 1N53 and MA 400 74 were used. At 90 and 67 GHz "Gordy type" point contact detectors were preferred because of the low microwave power level. Phase sensitive detection was performed by an Ithaco Dynatrac 391 A.

A unique interpretation of collisional effects is often complicated because the collisional transfer may result from cascaded collisional or higher order transitions [1, 20, 21]. To discriminate between the two possibilities we performed a triple resonance or "clamping" [20] experiment for the levels given in Figure 4. We take this experiment as an example for monitoring the transfer of population to the levels of the signal transition. The apparatus is drawn in Figure 5. In this experiment the radiation of three phase stabilised MW-sources had to be combined, which was facilitated by the stripline cell [19].

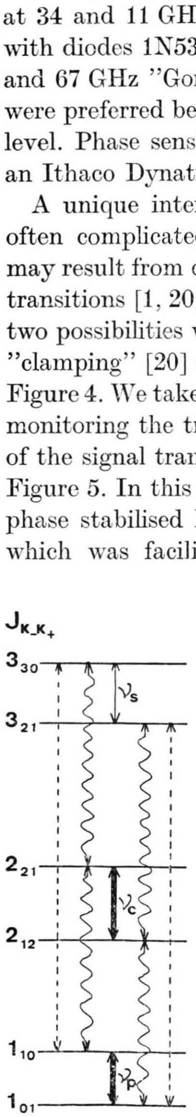

Fig. 4. Level scheme of the triple resonance or clamping experiment. ν_p modulated pump radiation, ν_c high power radiation for clamping or equilibrating the population of the 2_{12} and 2_{21} levels, ν_s signal radiation, ←〰→ dipolar collisional transitions, ←----→ higher order collisional transitions according to selection rules [1,2].

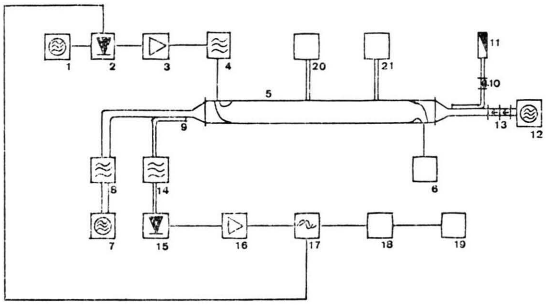

Fig. 5. Scheme of the triple resonance spectrometer for the clamping experiment. The pump radiation is on-off modulated, the signal is phase sensitive detected.

1 MW-sweeper X-band	11 detector for monitoring ν_c
2 PIN-modulator	12 MW-sweeper K-band
3 TWT-amplifier	13 waveguide isolators
4 low pass filter	14 band pass filter 18–26 GHz
5 stripline cell, 1.5 m, X-band cross section	15 detector for signal
6 power meter	16 preamplifier
7 Klystron (OKI 35V12)	17 phase sensitive detector
8 band pass filter 26–40 GHz	18 signal averager
9 directional coupler 10 dB	19 recorder
10 attenuator	20 capacitance manometer
	21 vacuum tank

Tab. 2. η-values of ethylene oxide measured by four level double resonance. U field free case. For the $|m|$-resolved values DC fields up to 2000 V/cm were applied. Temperature −40° C, Pressure 10 mT. Error estimated.

Signal transition	pump	η
$2_{21}-2_{12}$	$1_{10}-1_{01}$	%
U	U	$-\ 3.3\pm0.1$
$\lvert m\rvert=1$	$\lvert m\rvert=1$	$-\ 1.1\pm0.1$
$\lvert m\rvert=2$	$\lvert m\rvert=1$	$-\ 3.8\pm0.1$
$1_{10}-1_{01}$	$2_{21}-2_{12}$	
U	U	-44.1 ± 0.3
$\lvert m\rvert=1$	$\lvert m\rvert=1$	-11.0 ± 0.5
$\lvert m\rvert=1$	$\lvert m\rvert=2$	-33.7 ± 0.5
$2_{12}-1_{01}$	$2_{21}-1_{10}$	
U	U	$-\ 6.0\pm0.5$
$m=0$	$m=0$	~ 0
$m=0$	$\lvert m\rvert=1$	$-\ 5.2\pm0.7$
$\lvert m\rvert=1$	$m=0$	$-\ 5.5\pm0.7$
$\lvert m\rvert=1$	$\lvert m\rvert=1$	~ 0
$2_{21}-1_{10}$	$2_{12}-1_{01}$	
U	U	$-\ 4.0\pm0.5$
$m=0$	$m=0$	~ 0
$m=0$	$\lvert m\rvert=1$	$-\ 2.9\pm0.5$
$m=0$	$m=0$	$-\ 3.2\pm0.5$
$\lvert m\rvert=1$	$\lvert m\rvert=1$	~ 0

A Klystron OKI 35 V 12 was the source for the clamping radiation. We tested that the output power was sufficient to equilibrate the population for a pressure of about 10 mT by an experiment of the type of Figure 1c. As the MMDR-signal of the $3_{30}-3_{21}$ transition is weak and may be disturbed by the dynamic Stark effect [22, 23]* the collisional signal was taken as the difference of signals with the clamping radiation on and off resonant. To increase the sensitivity the PSD was followed by an averager (Fabri-Tek 1072).

Results of the Four Level Double Resonance Experiments

The results of the double resonance experiments are listed in Table 2. The η-values are given for m-unresolved and $|m|$-resolved conditions. The m-degeneracy was lifted by DC-fields up to 2000 V/cm. The DC- and MW-field were parallel. Consequently the spectroscopic selection rule of the signal transition was $\Delta m=0$.

The negative sign of η indicates a decrease of the signal absorption I when the pump radiation is resonant. The pressure was 10 mT. It has been checked that the η-value was nearly insensitive to pressure variation in this region if saturation was maintained. An example is given in Figure 6.

As can be seen from Table 2 the η-values are $|m|$-dependent.

In the triple resonance experiment a signal was observed of the $3_{30}-3_{21}$ transition for off resonant

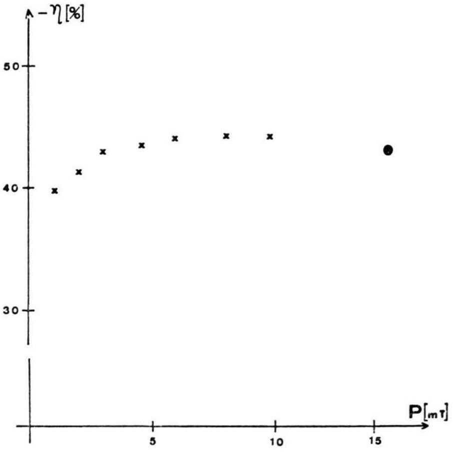

Fig. 6. Pressure dependence of η. As example, $2_{21}-2_{12}$ transition pumped, $1_{10}-1_{01}$ transition monitored. ● pump power was not sufficient for saturation. For analysis the η-value was taken from the plateau region.

---

* A method to eliminate most of the influence of the dynamic Stark effect will be published later.

clamping radiation. After tuning the clamping radiation to resonance with the $2_{21}-2_{12}$ transition the $3_{30}-3_{21}$ line signal disappeared. This shows that the $3_{30}-3_{21}$ collision induced signal is predominantly a cascaded one. This supports our initial assumption of the predominance of dipolar collision induced transitions or rate constants k_{ij}.

Experimental and Apparatus for the Time Domain Measurements

For the time domain measurements of T_1 and T_2 we used the transient Stark-switch technique [4, 6, 24, 25]. T_1 was determined by π, τ, $\pi/2$-experiments described by Mäder et al. [6] using a Boxcar integrator (PAR 162/164). For T_2 the decay of the transient emission was recorded by a waveform recorder (Biomation 6500). The analysis was carried out by means of a computer (PDP 11/10 or Texas Instruments TI 990/10). For the frequencies of 67 and 90 GHz a cell of 1.5 m length was used for better transmission. The "Gordy-type" point contact detectors had a sufficient time responce.

To account for a possible $|m|$-dependence of the relaxation time T_1, the experiments were performed with π, τ, $\pi/2$-pulse sequences given in Figure 7. For the π, τ, $\pi/2$-pulse sequence of Fig. 7a the microwave radiation ν is resonant with one $|m|$-component of the transition. In the period before the polarizing π-pulse the transition is degenerate and ν is off resonant. The π-pulse polarizes one single $|m|$-component and inverts the population difference of the m-levels. The degenerate system then relaxes under field free conditions. The probing for relaxation to thermal equilibrium by the $\pi/2$-pulse is again under resonance condition with one $|m|$-component.

To investigate the relaxation for one single $|m|$-component a π, τ, $\pi/2$-pulse sequence with an DC voltage is used as shown in Figure 7b. The electric DC-voltage for $|m|$-resolved conditions was applied to the Stark septum.

In a third version the microwave ν is resonant to the degenerate transition. So the π-pulse polarizes all $|m|$-components together. The relaxation to equilibrium occurs in presence of a DC-field, the probing is again under zero field conditions. T_2-measurements were made by observing the decay following a $\pi/2$-pulse. To avoid "fast passage" [4, 25] the microwave was adjusted to be resonant to the $|m|$-component with the largest Stark shift. Fourier transform spectroscopy [10] is another method to determine T_2 with MW-pulses instead of Stark-switch.

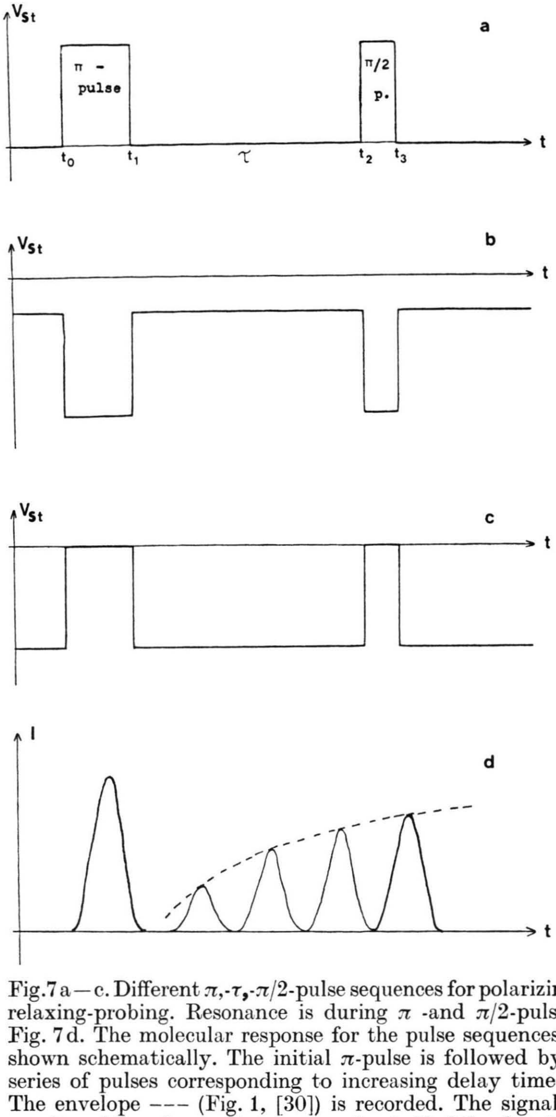

Fig. 7a–c. Different π,-τ,-$\pi/2$-pulse sequences for polarizing-relaxing-probing. Resonance is during π -and $\pi/2$-pulses. Fig. 7d. The molecular response for the pulse sequences is shown schematically. The initial π-pulse is followed by a series of pulses corresponding to increasing delay time τ. The envelope --- (Fig. 1, [30]) is recorded. The signal is monitored by a boxcar integrator after half of the duration of a π-pulse (corresponding to a $\pi/2$-pulse) [6, 30].

Results of the Time Domain Experiments

The pressure dependence of T_1 and T_2 is given in Table 3 by the slope β from

$$\frac{1}{T_{1,2}} = \alpha_{1,2} + \beta_{1,2}\, p\,.$$

Transition $J_{K_-K_+} - J'_{K_-'K_+'}$	$\lvert m \rvert$	T_1 β [MHz/$m\,T$]	DC-field [V/cm]	Method	T_2 β [MHz/$m\,T$]
$1_{10} - 1_{01}$	U	0.157(4)	0	7c	
	1	0.161(2)	0	7a	
	1	0.160(3)	200	7b	
	1	0.163(3)	600	7b	0.157(1)
$2_{21} - 2_{12}$	U	a			
	1	0.160(2)	1000^{b}	7b	
	2	0.157(5)	0	7a	
	2	0.160(5)	500	7b	0.151(5)
$2_{12} - 1_{01}$	U	0.162(2)	0	7c	
	0	0.169(5)	1000^{b}	7b	
	1	0.161(4)	0	7a	0.168(1)
$2_{21} - 1_{10}$	U	0.185(6)	0	7c	
	0	0.194(5)	0	7a	
	1	0.186(7)	0	7a	0.174(3)

Tab. 3. T_1- and T_2-measurements of ethylene oxide, C_2H_4O, from a range of 1 to 15 mT pressure p, temperature −40° C. Listed is β from $1/T = \alpha + \beta p$. In brackets standard error in units of the last digit. *U m*-unresolved. DC-field and method see Figure 7.

[a] could not be measured as available Starkfield (450 V) was not high enough to seperate Stark satellites sufficiently from the line.

[b] DC voltage was necessary to split $\lvert m \rvert$-component more than 1,2 MHz from the other $\lvert m \rvert$-components.

Tab. 4. T_1 measurements of ethylene oxide in a mixture with hydrogen H_2 1.5 to 25 mT. H_2 with 3,3 mT C_2H_4O. Temperature −40° C. Listed is γ from $1/T_1 = \beta\, p_{C_2H_4O} + \gamma p_{H_2} + \alpha$. See also Table 3.

Transition $J_{K_-K_+} - J_{K_-K_+}$	$\lvert m \rvert$	γ [MHz/mT]	T_1 DC-field [V/cm]	Method
$2_{21} - 2_{12}$	1	0.053 (3)	1000	7b
	2	0.049 (2)	1000	7b
	2	0.047 (1)	0	7a

A comparison of the results of the experiments with different conditions shows that there is no significant difference. Further the T_2- and T_1-values agree within experimental accuracy. In addition Table 4 gives T_1 measurements of ethylene oxide in mixtures with hydrogen. In all our experiments T_1 is nearly the same for different $\lvert m \rvert$-transitions.

Theory

We want to interpret the experimental results for the m-degenerate transitions in terms of the molecular interaction on the basis of Equation (1)* [7, 26]:

$$i \frac{\partial \varrho_{fi}}{\partial t} = \frac{1}{\hbar} [H + K, \varrho]_{fi} - i \sum_{f'i'} \Lambda_{fi,f'i'} \cdot \varrho_{f'i'} \,. \quad (1)$$

ϱ is an element of the density matrix, H the hamiltonian of the isolated monitored molecule, K describes the interaction of the molecule with the electromagnetic field, $\Lambda_{fi,f'i'}$ are elements of the relaxation superoperator Λ, which can be expressed in terms of the S-matrix. (1) was derived under the assumption of the impact approximation [7, 26]. Only binary collisions of the monitored molecule with perturber molecules are considered. The collision time has to be short with respect to the mean time between collisions and the inverse frequency offset $(\omega - \omega_0)$.

The element $\Lambda_{ii,jj}$ connects diagonal elements ϱ_{ii} and ϱ_{jj} of the density matrix ϱ. So $\Lambda_{ii,jj}$ may be interpreted as the rate constant k_{ji} describing population transfer from level j to i.

$$\Lambda_{ii,jj} = - k_{ji}{}^{**} \quad (2)$$

$\Lambda_{ii,ii}$ gives the total rate of transfer out of level i. So

$$\Lambda_{ii,ii} = \sum_{j \neq i} k_{ij} \,. \quad (3)$$

The element $\Lambda_{ij,ij}$ $(i \neq j)$ connects ϱ_{ij} to itself and describes a loss of the radiation induced coherence (T_2-relaxation) [7]. The $\Lambda_{ij,kl}$ $(i \neq j)$ coupling off diagonal ϱ_{ij} to off or on diagonal ϱ_{kl}, are usually set to be zero, which means that no collisional trans-

---

* Correctly we should use for (1) the equation for degenerate systems (Eqs. 4.16 and 4.17 of [7]). As our Eqs. (13) and (14) would be of the same form we omit the superscript ^{0} denoting the tensorial charactor of Λ.

** Also the rate constants are averages over the vibronic groundstate and Maxwellian velocity distribution. So the k_{ij} depend on temperature.

fer of coherence between pairs of levels is assumed [27, 28]*. In the following only linear polarized free space MW-radiation is considered. The effects of translation perpendicular to the MW-field are neglected [30]. The errors of these simplifications are within experimental accuracy. From (1) and (2)

$$\left(\frac{\partial}{\partial t}\varrho_{ii}\right)_{\text{relax.}} = \sum_j k_{ji}\,\varrho_{jj} \tag{4}$$

may be derived for the relaxation. The sum extends over all occupied levels. This reduction reflects the experimental conditions. The probing signal radiation is permanently present, but assumed to be small enough not to disturb the relaxation processes.

(4) is equivalent to the linear rate equations used for the analysis of four level double resonance experiments [1]. With the number density N and $N \cdot \varrho_{ii} = n_i$ the occupation number of level i (4) modifies for thermal equilibrium (superscript ^{0}) to

$$\dot{n}_i{}^0 = \sum_{j \neq i} (k_{ji}\, n_j{}^0 - k_{ij}\, n_i{}^0) = 0 \tag{5}$$

without pump radiation.

With the pump radiation resonant with the levels 1 and 2 (Fig. 1b) and equilibrating $n_1 = n_2$ by saturation** the steady state equation from (4) is

$$\dot{n}_i = \sum_{j \neq i} (k_{ji}\, n_j - k_{ij}\, n_i) = 0$$

with non-Boltzmann n_m. For the levels 3 and 4 (Fig. 1b) (5) and (6) combine to

$$\begin{aligned} \delta\dot{n}_i &= \sum_{j \neq i} (k_{ji}\,\delta n_j - k_{ij}\,\delta n_i) = 0\,, \\ i &= 3, 4\,, \end{aligned} \tag{7}$$

with $\delta n_m = n_m - n_m^0$, the deviation from equilibrium induced by radiation. For the signal transition $3 \leftrightarrow 4$ we have:

$$\eta = \frac{\Delta I}{I} = \frac{\delta n_4 - \delta n_3}{n_4{}^0 - n_3{}^0}\,. \tag{8}$$

Under certain approximations $\delta n_4 - \delta n_3$ may be related to $\delta n_2 - \delta n_1$. Only population changes δn_l within the four levels are retained treating all other levels as a thermal bath. The sum (7) over occupied levels j reduces to

$$\begin{aligned} &k_{13}\,\delta n_1 + k_{23}\,\delta n_2 + k_{43}\,\delta n_4 \\ &\qquad - \sum_j k_{3j}\,\delta n_3 = 0\,, \\ &k_{14}\,\delta n_1 + k_{24}\,\delta n_2 + k_{34}\,\delta n_3 \\ &\qquad - \sum_j k_{4j}\,\delta n_4 = 0\,. \end{aligned} \tag{9}$$

As for rotational levels $e^{-(E_j - E_i)/kT} \approx 1$ for usual temperatures

$$k_{ij} = k_{ji} \tag{10}$$

by the principle of detailed balance [7].

With the collisional selection rules [2] for ethylene oxide and the result of the triple resonance experiment, the rate constants are limited to first order dipolar type. (9) reduces then to

$$\begin{aligned} &k_{13}\,\delta n_1 + k_{34}\,\delta n_4 - k_{13}\,\delta n_3 - k_{34}\,\delta n_3 \\ &\qquad - k_3\,\delta n_3 = 0\,, \\ &k_{24}\,\delta n_2 + k_{34}\,\delta n_3 - k_{24}\,\delta n_4 - k_{34}\,\delta n_4 \\ &\qquad - k_4\,\delta n_4 = 0 \end{aligned} \tag{11}$$

with

$$k_i = \sum_{j \neq 1,2,3,4} k_{ij}\,, \quad i = 1, 2, 3, 4$$

as bath constants. Using Eq. (11) $\delta n_4 - \delta n_3$ may be related to $\delta n_2 - \delta n_1$. As for saturation

$$\delta n_2 = -\,\delta n_1 = \frac{n_1{}^0 - n_2{}^0}{2} \tag{12}$$

we have:

$$\eta = -\frac{\nu_p}{2\,\nu_s}\exp[(E_3 - E_1)/k\,T]\,\frac{k_{13}k_4 + k_{24}k_3 + 2\,k_{13}k_{24}}{k_3(k_{24} + k_{34}) + k_4(k_{13} + k_{34}) + k_3 k_4 + k_{24}k_{34} + k_{13}k_{34} + k_{13}k_{24}}\,. \tag{13}$$

η is related to rate and bath constants for zero DC-field. (13) applies for pump transition $1 \leftrightarrow 2$ and signal transition $3 \leftrightarrow 4$*** as given in Figure 1 b. The other cases of Fig. 1c, 1d, 1e derive with (10) by the substitution given in Table 5. From (13) (and the three other analogous equations) and $k_{ij} > 0$, $k_i > 0$ theory predicts η to be negative. The signal intensity I decreases when the pump radiation is applied. This agrees with the experimental results of Table 2.

---

* Transfer of coherence is discussed in [29].

** It was proved by time resolved four level double resonance, that with a 33 kHz modulation saturation and steady state is achieved.

*** A convenient method for solving (11) for (8) is the network analysis [9, 31, 32].

Tab. 5. Substitution of indices of rate and bath constants for the cases of Figures 1 b–e.

1 b	1 c	1 d	1 e
1	4	1	2
2	3	3	4
3	2	2	1
4	1	4	3

By Liu et al. [7] the relaxation time T_1 has been related to the elements of the relaxation superoperator Λ for linear molecules. It has been shown [10] that an extension to asymmetric top molecules is possible. Our analysis for the rate constants k_{ij} will be based on the results of the π, τ, $\pi/2$-sequence of Figure 7 c. In this case the degenerate transition was polarized. As we found experimentally no m-dependence of T_1, this choice is not critical. So we take Eq. (3–37) from Liu, where i and f now indicate asymmetric rotor levels.

$$\frac{1}{T_1} = \frac{1}{2}\left(\Lambda_{ii,ii} - \Lambda_{ff,ii} + \Lambda_{ff,ff} - \Lambda_{ii,ff}\right) . \qquad (14)$$

With the identification $i = 1$ and $f = 2$ according to Fig. 1 b, (2), (3) and (10) we get

$$\left(\frac{1}{T_1}\right)_{1\leftrightarrow 2} = \frac{1}{2}\left(k_1 + k_2 + 4\,k_{12} + k_{13} + k_{24}\right) . \qquad (15)$$

For the other transitions according to Figs. 1 c–e the relations are derived by use of the substitutions of Table 5. The final numerical analysis for the k_{ij} and k_i was based on the pressure dependence β of T_1 as listed in Table 3.

Analysis and Discussion

For the determination of four rate and four bath constants we have eight non-linear equations from the relations (13), (15) and analogous ones. These equations are related to the change of diagonal elements of the density matrix as can be seen from Eqs. (1), (4) and (6).

A computer program using a Marquardt procedure [33] was written to solve the non-linear problem. The solutions were limited $k_{ij} \geqq 0$ and $k_i \geqq 0$.

We obtained for the k_{ij} and k_i two sets of solutions, which are compatible with the eight non-linear equations with minimum deviation. They are given in Table 6. To check an approximation which had been used [1, 20] we set some bath constants equal to each other. First we set $k_3 = k_4$ and second $k_1 = k_2 = k_3 = k_4$. As can be seen from Table 6, these conditions influence the values for the constants k_{ij} and k_j*.

Tab. 6. Rate and bath constants [kHz/mT] of Fig. 1 a for ethylene oxide. In brackets error estimated from experimental uncertainties by variing input data. a, b two solutions without restrictions, c for $k_3 = k_4$, d, e for $k_1 = k_2 = k_3 = k_4$.
f, g for $|m| = 1$ subsystem without restrictions (rate and bath constants differ by definition from those of column a to e).

	a	b	c	d	e	f	g
k_{12}	10(3)	3(1)	8	5	6	~0	~0
k_{13}	3(2)	26(1)	29	11	13	6	2
k_{24}	33(2)	10(3)	7	22	24	15	16
k_{34}	3(1)	9(3)	12	58	67	~0	~0
k_1	182(2)	68(13)	76	136	130	149	167
k_2	65(2)	210(3)	209	136	130	157	153
k_3	116(16)	142(15)	120	136	130	147	152
k_4	159(10)	108(3)	120	136	130	156	159

Summarizing the analysis, we may state that the dipolar contribution to relaxation is the most important one. This is in agreement with the collisional selection rules [2] and the results of this work. It agrees further with the observation that a double resonance experiment in a magnetic field with the pump radiation resonant to $1_{10} - 1_{01}$ ($m = \pm 1$) and the signal radiation resonant to $2_{21} - 2_{12}$ ($m = \mp 1$) gave no collision induced signal, although the transition is allowed by quadrupole collisional selection rules.

We noticed that the η-values of Table 2 for unresolved (U) and m-resolved conditions are related to each other. The superscript of I, ΔI and η signifies the signal, the subscript the pump level by $|m|$.

For the signal transition $1_{10} - 1_{01}$ and the pump transition $2_{21} - 2_{12}$ the relation is:

$$\eta_u = \frac{\Delta I_u}{I_u} = \frac{\Delta I_1^1 + \Delta I_2^1}{I^1} = \eta_1^1 + \eta_2^1 . \qquad (16)$$

From Table 2 we obtain $\eta_u = -44.7 \pm 0.5\%$ which compares with a measured value $-44.1\% \pm 0.3\%$. For the reverse case with signal transition $2_{21} - 2_{12}$ and pump transition $1_{10} - 1_{01}$, we have

$$\eta_u = \frac{\Delta I_u}{I_u} = \frac{\Delta I_1^1 + \Delta I_1^2}{I^1 + I^2} = \frac{\eta_1^1 I^1 + \eta_1^2 I^2}{I^1 + I^2} \qquad (17)$$

* As from the 1_{01}- and 1_{10} -levels besides k_{13} and k_{24} no other dipole channels emerge, we set $k_1 = k_2 = 0$ and got the physically unreasonable result $k_{34} \simeq 0$.

with the relative theoretical peak intensities $I^1 = 1$, $I^2 = 4$ we get

$$\eta_u = \frac{(-1.1)\cdot 1 + (-3.8)\cdot 4}{5} = -3.26 \pm 0.2\%$$

which compares with the measured value $-3.3 \pm 0.1\%$.

Our experimental data for the $|m|$-resolved conditions are not sufficient to determine the 19 rate and 10 bath constants for the 10 levels which develop under the influence of an electric field from the degenerate four level system of Figure 1.

Taking the Eq. (13), (15) and analogues as valid for the four level $|m| = 1$ subsystem the rate and bath constants of Table 6 column *f*, *g* were calculated. It can be seen that the constants change with respect to the unresolved conditions. We found it noticeable that with this set, the $|m|$-dependent η and the $|m|$-independent T_1 can be reproduced. The rate constants $k_{12} \sim 0$ and $k_{34} \sim 0$ of Table 6 column *f*, *g* agree with $\eta \sim 0$ of Table 2 for $|m| = 1$ of signal $2_{12} - 1_{11}$, and pump $2_{21} - 1_{10}$ and the reverse experiment. Because of the lack of experimental information on the other $|m|$-resolved transitions the rate and bath constants for resolved and unresolved conditions cannot be related to each other. Further work will be necessary.

We thank the Deutsche Forschungsgemeinschaft and the Fonds der Chemie for funds, one of us (W. Sch.) for a doctoral fellowship of the Studienstiftung des deutschen Volkes. We kindly aknowledge many discussions with the members of our group, especially Dr. Mäder also for critically reading the manuscript.

[1] T. Oka, Advan. At. Mol. Phys. **9**, 127 (1973).
[2] H. Dreizler and W. Schrepp, Z. Naturforsch. **33a**, 197 (1978).
[3] J. I. Steinfeld and P. L. Houston in J. I. Steinfeld (Ed.) Laser and Coherence Spectroscopy, Plenum Press, New York 1978, p. 1 ff.
[4] J. C. McGurk, T. G. Schmalz and W. H. Flygare, Adv. Chem. Phys. **25**, 1 (1974).
[5] R. H. Schwendeman, Ann. Rev. Phys. Chem. **29**, 537 (1978).
[6] H. Mäder, W. Lalowski and R. Schwarz, Z. Naturforsch. **34a**, 1181 (1979).
[7] W. K. Liu and R. A. Marcus, J. Chem. Phys. **63**, 272 (1975); J. Chem. Phys. **63**, 290 (1975).
[8] V. Prakash and J. E. Boggs, J. Chem. Phys. **57**, 2599 (1972).
[9] R. M. Lees and S. S. Haque, Can. J. Phys. **52**, 2250 (1974).
[10] W. Schrepp, G. Bestmann, and H. Dreizler, Z. Naturforsch. **34a**, 1467 (1979); W. Schrepp, Thesis, Kiel 1980.
[11] R. H. Schwendeman and T. Amano, J. Chem. Phys. **70**, 962 (1979).
[12] H. Mäder, W. Schrepp, and H. Dreizler, Z. Naturforsch. **31a**, 1419 (1976).
[13] R. M. Lees, Can. J. Phys. **56**, 1417 (1978).
[14] W. E. Hoke, D. R. Bauer, and W. H. Flygare, J. Chem. Phys. **67**, 3454 (1977).
[15] J. B. Cohen and E. B. Wilson, J. Chem. Phys. **58**, 456 (1973).
[16] W. Schrepp and H. Dreizler, Z. Naturforsch. **34a**, 903 (1979).
[17] O. Stiefvater, Z. Naturforsch. **30a**, 1756 (1975).
[18] J. Ekkers, A. Bauder, and Hs. H. Günthard, Rev. Sci. Instrum. **45**, 311 (1974).
[19] H. Dreizler, W. Schrepp, and R. Schwarz, Z. Naturforsch. **34a**, 571 (1979).
[20] R. M. Lees and T. Oka, J. Chem. Phys. **49**, 4234 (1968).
[21] M. R. Verter and H. A. Rabitz, J. Chem. Phys. **59**, 3816 (1973).
[22] S. H. Autler and C. H. Townes, Phys. Rev. **100**, 703 (1953).
[23] P. Glorieux, J. Legrand, B. Macke, and J. Messelyn, JQRST **12**, 731 (1972).
[24] H. Mäder, J. Ekkers, W. Hoke, and W. H. Flygare, J. Chem. Phys. **62**, 4380 (1975).
[25] H. Mäder, H. Bomsdorf, and U. Andresen, Z. Naturforsch. **34a**, 850 (1979).
[26] C. Cohen-Tannoudji in Frontiers in Laser Spectroscopy, Vol. 1. Les honches 1975, Session XX VII, North Holland Publ. Comp. Amsterdam 1977, p. 7 ff.
[27] B. Macke, P. Glorieux, and F. Rohart, Phys. Lett. **62A**, 23 (1976).
[28] S. Stenholm, J. Phys. B **10**, 761 (1977).
[29] F. Rohart, B. Segard, and B. Macke, J. Phys. B: Atom Molec. Phys. **12**, 3891 (1979).
[30] H. Mäder, Z. Naturforsch. **34a**, 1170 (1979).
[31] R. M. Lees and T. Oka, J. Chem. Phys. **51**, 3027 (1969).
[32] J. Schnakenberg, Rev. Mod. Phys. **48**, 571 (1976).
[33] D. W. Marquardt, An Algorithm for the Least Squares Estimation of Nonlinear Parameters, SIAM Journal, Vol. 11, June 1963.
[34] D. H. Sutter, Z. Naturforsch. to be published.